Impact of Water Mist on Chemical Reaction of Methane/air/water-mist Premixed Flames

Seiya Nakanishi, Yasuhiro Ogami, Masahiro Ito and Takashi Tsuruda
Faculty of Systems Science and Technology, Akita Prefectural University
Yurihonjyo, Akita, Japan

1 Introduction

Water-mist is receiving tremendous attention as one of the latest types of fire extinguishers as a substitute for halon. There have been numerous studies on extinguishing fire by water-mist for several decades (e.g. [1, 2]). Fundamental studies have also been conducted to elucidate the mechanisms of fire suppression and extinction by water-mist addition, with the focus being mainly on diffusion flames. Naito et al. [3], Yoshida et al. [4], and Sasongko et al. [5] performed experimental studies using a counter-flow diffusion flame. Lentati and Chelliah [6, 7] conducted numerical simulations considering the water droplet behavior. In regard to premixed flames, Blouquin and Jouline [8] theoretically studied the flame inhibition effect of mono-disperse water-mist by focusing on the effect of the droplet diameter on the flame speed. Kee et al. [9] conducted numerical simulations taking into consideration the detailed chemical reaction mechanism, in which the flame speed exhibited the same trend as displayed in the study by Blouquin and Jouline [8]. Fuss et al. [10] measured the flame speeds of stoichiometric CH_4/air/water-mist premixed flames. These studies were conducted only under a narrow range of equivalence ratios and low water-mist concentrations. Generally, premixed flames allow reaction control and are suitable to analyze the effect of water-mist on the chemical reaction. However, the experimental data were insufficient for verification of the existent chemical reaction mechanisms under the conditions with water-mist.
Recently, Ogami et al. [11] measured the flame speeds under the condition of high water-mist concentrations and a wide range of equivalence ratios. In this study, further experiments were conducted for CH_4/air/water-mist premixed flames. Numerical simulations considering the detailed chemical reaction mechanisms were conducted and compared with experimental data. Furthermore, the effects of water-mist on the chemical reaction were elucidated via a sensitivity analysis.

2 Experimental Method

Figure 1 shows the schematic of the experimental setup. The experimental apparatus consists of a water supply system, water-mist generator, circular nozzle burner with an extension tube, and flame holder. Distilled water is continuously supplied to the water-mist generator so that the water level is constant.

Correspondence to: ogami@akita-pu.ac.jp

Water-mist is formed using the ultrasonic transducer that is placed at the bottom of the water-mist generator. Air and CH_4, whose flow rates are controlled by the mass flow controllers, are supplied from the upper part of the water-mist generator. A gas/liquid two-phase flow is introduced to the extension tube. Several types of extension tubes with different cross-sectional areas were employed. Consequently, it was possible to vary the mass fraction of water-mist [11]. The gas/liquid two-phase flow is supplied to the circular nozzle burner whose exit diameter and nozzle contraction ratio are 12 mm and 10, respectively. A pilot flame is formed around the burner lip to strengthen the flame base and prevent blow-off. The amount of premixed gases supplied for the pilot flame is less than 10% of the main premixed flame. The burner exit is enclosed with a cubic cover made of quartz glass to separate the hot combustion gas and surrounding cold gas. Consequently, it became possible to restrain the influence of the disturbances and buoyancy caused by the surrounding cold gas, and to exclude the effect of the outer flame on of the characteristics of the inner premixed flame in fuel-rich conditions. All the devices were placed on an electronic balance, and the mass flow rate of water was measured prior to the combustion experiments.
The mass fraction of water, Y_{H_2O}, is defined as the ratio of the mass of added water that contains both the saturated vapor and water-mist (i.e., the liquid phase) to the total mass of the gas/liquid two-phase mixture. The burning velocities are obtained by the area method for equivalence ratios (ϕs) ranging from 0.5 to 1.5 and $Y_{H_2O} = 0.00$ to 0.07.

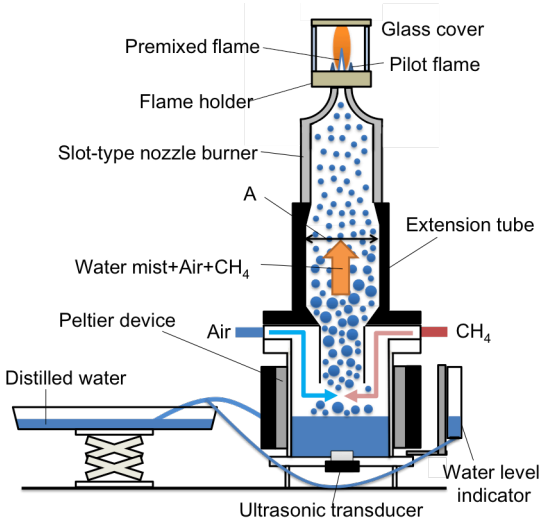

Figure 1. Schematic of the experimental apparatus.

3 Numerical Method

The numerical simulations were conducted using the PREMIX code [12] of the CHEMKIN-PRO package [13]. Water-mist (i.e., the liquid phase) was defined as the water-mist gas (WMG) based on the method of Takahashi et al. [14]. In this method, the liquid phase of H_2O was treated as an ideal gas with 1354 times the molecular weight of H_2O and having the same thermodynamic properties as liquid water. The evaporation of the WMG was modeled by an Arrhenius-type chemical reaction, i.e., $WMG \rightarrow 1354H_2O(gas)$, so that it was possible to consider both the latent and sensible heat associated with the WMG. The Arrhenius parameters of the WMG reaction were set to complete the evaporation at the gas temperature of 500 K. Therefore, it was assumed that the WMG completely evaporated in the preheating zone and did not affect the chemical reaction in the reaction zone. Such an assumption is considered valid because the complete evaporation of water-mist in the preheating zone was confirmed in

the all conditions tested in this study [11]. The laminar flame speeds of the CH_4/air/water-mist premixed flames were calculated using the detailed chemical reaction mechanisms of GRI-Mech 3.0 [15], San Diego Mech. [16], and USC Mech. [17] for the same equivalence ratio range and water mass fraction as those in the experiments.

4 Flame Speed of CH_4/Air/Water-Mist Premixed Flame

Figures 2(a)–(c) show the experimental results of the flame speed, S_u, as a function of Y_{H_2O} for the equivalence ratio of 0.8, 1.0, and 1.3, respectively. The experimental data are fitted by an approximated curve based on the analytical result obtained by Blouquin and Jouline [8,11]. In Fig. 2, the numerical results using several detailed chemical reaction mechanisms are also shown and compared with the experimental results. The values of Y_{H_2O} in the numerical results are limited to 0.07 or less owing to the insufficient convergence in the conditions with high Y_{H_2O}. The sudden change in the decreasing trend of S_u after $Y_{H_2O} \approx 0.02$ is a result of the existence of the liquid phase, i.e., when $Y_{H_2O} \leq 0.02$, only the gas phase exists, and when $Y_{H_2O} > 0.02$, both the gas and liquid phases are present.

The numerical results for $\phi = 1.3$ are marginally in good agreement with the experimental results. In the case of $\phi = 0.8$, the decreasing trend of S_u of the numerical results is similar to that of experimental

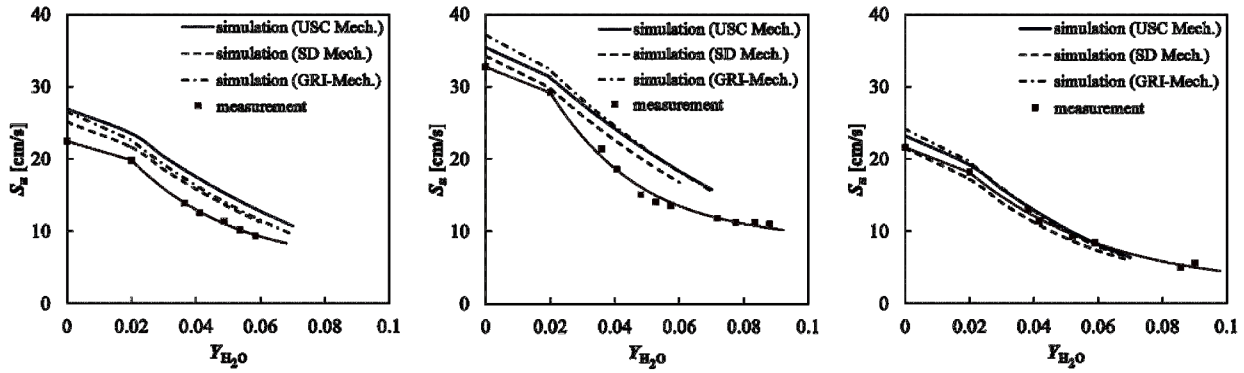

(a) $\phi = 0.8$ (b) $\phi = 1.0$ (c) $\phi = 1.3$

Figure 2. Flame speed as a function of water mass fraction (symbol: experiment, line: simulation).

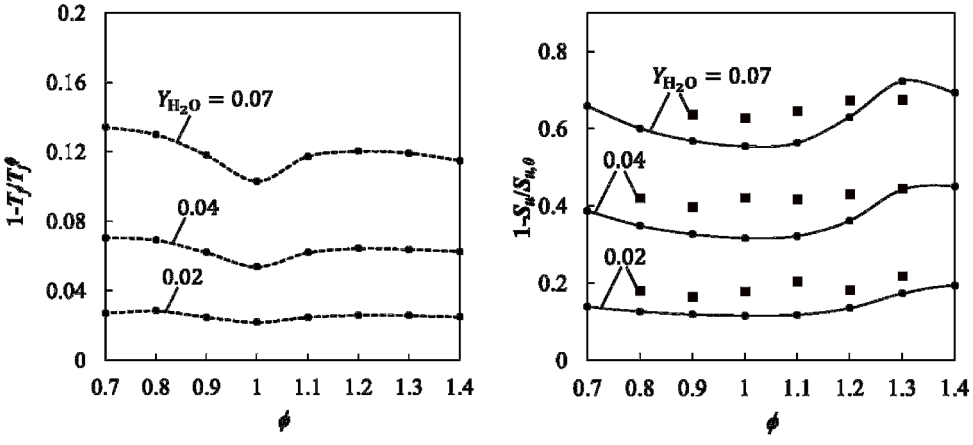

(a) temperature (b) flame speed

Figure 3. Reduction ratio as a function of equivalence ratio (symbol: experiment, line: simulation).

results, while the values of S_u of the numerical results are much larger than experimental results under all Y_{H_2O}. In the case of ϕ = 1.0, the numerical results of S_u for San Diego Mech. [16] are in good agreement with experimental data when $Y_{H_2O} \leq 0.02$, but there is a major discrepancy in the decreasing trend of S_u of numerical results in the condition of $Y_{H_2O} > 0.02$. The experimental S_u data fitted by the approximate curves have large convex curvatures when going downward for ϕ = 1.0, although S_u decreases linearly after $Y_{H_2O} \approx 0.02$ in the case of numerical results. Such a difference in the decreasing trend will lead to an underestimation of S_u if a linear extrapolation was conducted using numerical results to estimate S_u at high Y_{H_2O}. Therefore, it is necessary to be careful when estimating the inhibition effect of water-mist on the flame speed for practical purposes by using the numerical results.

Figure 3(a) shows the reduction ratio of the maximum flame temperature, $1 - T_f/{T_f}^0$, where T_f and ${T_f}^0$ denote the maximum flame temperature with and without water-mist addition, respectively. Figure 3(b) displays the reduction ratio of S_u, $1 - S_u/{S_u}^0$, where ${S_u}^0$ denotes the flame speed without water-mist. The reduction ratio of T_f generally decreases as the equivalence ratio increases and becomes higher under the condition of higher Y_{H_2O}. The reduction ratio of S_u is expected to exhibit the same trend as that of T_f because S_u strongly depends on T_f. However, in both the experimental and numerical results, the reduction ratios of S_u and T_f exhibit different trends. In the case of experimental results, the reduction ratio of S_u monotonically increases as the equivalence ratio increases. In the case of numerical results, the reduction ratio of S_u first decreases in the lean condition and then increases in the rich condition. It is interesting to note that the reduction ratio of S_u for numerical simulation has a peak at $\phi = 1.3$ in the case of $Y_{H_2O} = 0.07$. This indicates that the flame speed of CH_4/air/water-mist flames depends not only on the flame temperature, but also on other factors. Because the chemical reaction is dominant in the premixed combustion, results in Fig. 3(b) suggest that water-mist has a significant impact on the chemical reaction, particularly under the rich condition.

As shown in Fig. 3(b), the difference of the reduction ratio of S_u between experimental data and numerical results becomes the largest at $\phi = 1.0$ in cases of $Y_{H_2O} = 0.04$ and 0.07. This is consistent with results seen in Fig. 2(b), i.e., the decreasing trend of S_u in numerical results have a large discrepancy at $\phi = 1.0$.

5 Effect of Water-Mist on the Chemical Reaction of CH_4/air/water-mist Premixed Flame

Figures 4(a) and (b) depict the sensitivity coefficients of the major elementary reactions for the cases of $Y_{H_2O} = 0.00$ and 0.07, respectively. In the case of $Y_{H_2O} = 0.00$ (Fig. 4(a)), the main chain-branching reaction, H + O_2 = O + OH (1), has the largest positive sensitivity at all the equivalence ratios. Reaction 31, CO + OH = CO_2 + H, has the second largest positive sensitivity particularly in the lean condition. The fall-off recombination reaction, H + O_2 (+M) = HO_2 (+M) (12), has the largest negative sensitivity in the lean condition; however, the magnitude of its sensitivity suddenly decreases as the equivalence ratio increases. The fall-off recombination reaction, CH_3 + M (+M) = CH_4 (+M) (88) has the largest negative sensitivity in the rich condition, and the magnitude of its sensitivity significantly increases as the equivalence ratio increases. This is because CH_4 has a high collision efficiency as a third body and promotes reaction 88 under the fuel rich condition. Such an increase in the sensitivity of reaction 88 causes an increase in the sensitivity of reaction 1 that competes with reaction 88 for H radical consumption in the rich condition.

In the case of $Y_{H_2O} = 0.07$ (Fig. 4(b)), reaction 88 becomes more dominant on the S_u decrease particularly in the fuel rich condition. This is because the collision efficiency of H_2O is much higher than other species, and reaction 88 is largely promoted by the water-mist addition. The sensitivity of reaction 1 also increases because of the enhancement of its competing reaction (i.e., reaction 88). The magnitude of the sensitivity

of reaction 12 is also increased by the water-mist addition; however, its increase is much smaller than that of reaction 88 and limited in the lean condition. The magnitude of the sensitivity of reaction 88 becomes the largest at $\phi = 1.3$. In this condition, the reaction rate of reaction 88 has a peak. This suggests that the reaction rate of reaction 88 reaches "fall off" because of high concentrations of H_2O and CH_4. Because reaction 88 has a small temperature dependency, reaction 88 becomes dominant even in the situation when the flame temperature is decreased by the water-mist addition. The peaks of the reduction ratio of S_u, observed in Fig. 3(b), at $\phi = 1.3$ are considered to be caused by the fall-off of reaction 88.

6 Conclusions

Measurements of the flame speeds of CH_4/air/water-mist premixed flames and numerical simulations considering the detailed chemical reactions were conducted under the conditions of a wide range of equivalence ratios and high water mass fractions. The numerical results of S_u differ significantly from the experimental results. The reduction ratio of S_u for the numerical simulation has a peak at $\phi = 1.3$ in the case of $Y_{H_2O} = 0.07$. This result indicates that water-mist has a significant impact on the fall-off reactions such

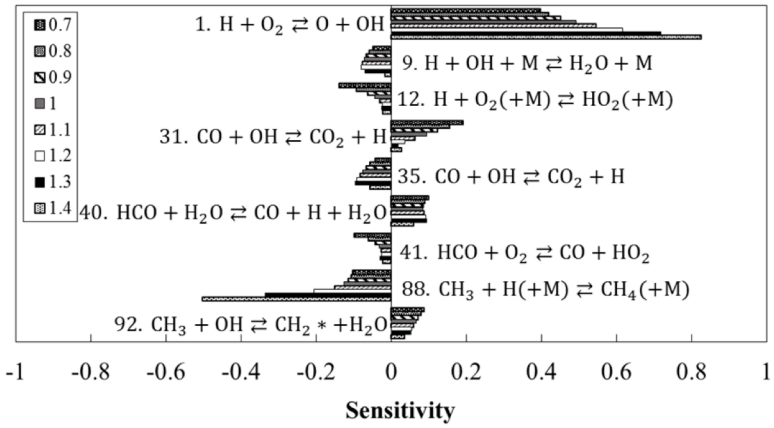

(a) $Y_{H_2O} = 0.00$.

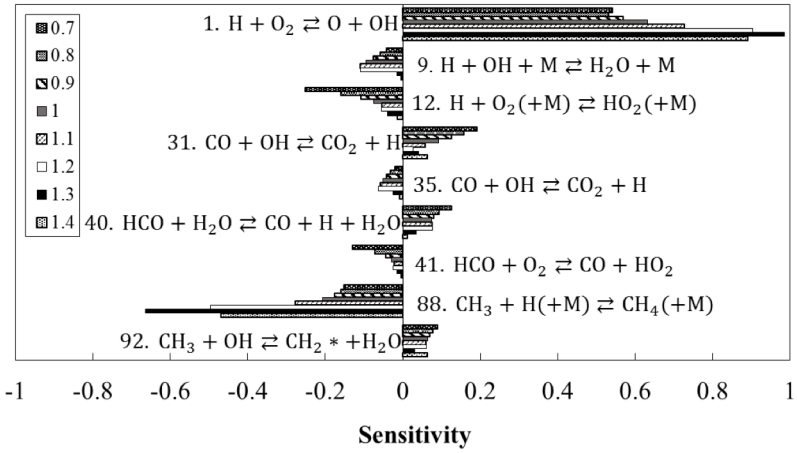

(b) $Y_{H_2O} = 0.07$.

Figure 4. Sensitivity coefficients (USC Mech. [15]).

as $CH_3 + M (+M) = CH_4 (+M)$, particularly in the rich condition because of the high concentration of third bodies such as H_2O and CH_4.

References

[1] Zhigang, L., et al. (2008). Cooling characteristics of hot oil pool by water mist during fire suppression. Fire Safety Journal. Vol. 43: 269-281.

[2] Liu, J., et al. (2013). Experimental Study on Ultra-fine Water Mist Extinguishing Heptane Cup Fire in Confined Space. Proc. Engineering. 52: 225-229.

[3] Naito, H., et al. (2011). Effect of fine water droplets on extinguishment of diffusion flame stabilized on the forward stagnation region of a porous cylinder. Proc. Combust. Inst. 33: 2563-2571.

[4] Yoshida, A., et al. (2015). Inhibition of counterflow methane/air diffusion flame by water mist with varying mist diameter. Fire Safety Journal 71: 217-225.

[5] Sasongko, M. N., et al. (2011). Extinction condition of counterflow diffusion flame with polydisperse water sprays. Proc. Combust. Inst. 33: 2555-2562.

[6] Lentati, A., and Chelliah, H. K. (1998). Physical, thermal, and chemical effects of fine-water droplets in extinguishing counterflow diffusion flames. Proc. Combust. Inst. 27: 2839-2846.

[7] Lentati, A., and Chelliah, H. K. (1998). Dynamics of Water Droplets in a Counterflow Field and their Effect on Flame Extinction. Proc. Combust. Flame. 115: 158-179.

[8] Blouquin, R., Joulin, G. (1998). On the quenching of premixed flames by water sprays: influences of radiation and polydispersity. Proc. 27th Symp. (int.) Combust.: 2829-2837.

[9] Yang, W., Kee, R.J. (2002). The effect of monodispersed water mists on the structure, Burning velocity, and extinction behavior of freely propagating, stoichiometric, premixed, methane-air flames. Combust. Flame 130: 332-335.

[10] Fuss, S.P., et al. (2002). Inhibition of premixed mehane/air flames by water mist. Proc. Combust. Inst. 29: 361-368.

[11] Ogami, Y., et al. (2016). A Study of Flame Inhibition Effects of High-Concentration Water Mist on CH_4/air Premixed Flames. Journal of Combustion Society of Japan. Vol.58. 183: 49-59 (in Japanese).

[12] Kee, R. J., Grcar, J, F., Smooke, M. D., Miller, J. A., and Meeks, E. (1998). Premix: A FORTRAN Program for Modeling Steady Laminar One-Dimensional premixed Flames. Sandia National Laboratories Report.

[13] Reaction Design, (2011). "CHEMKIN-PRO 15112", Reaction Design, Inc., San Diego.

[14] Takahashi, F., and Katta, V. (2009). Extinguishment of diffusion around a cylinder in a coaxial air stream with dilution or water mist. Proc. Combust. Inst. 32: 2615-2623.

[15] Smith G., et al. GRI-mech release 3.0: http://www.me.berkeley.edu/gri-mech/.

[16] Williams, F. A., et al. (2011). http://web.eng.ucsd.edu/mae/groups/combustion/mechanism.html.

[17] Wang H, et al. (2007). USC Mech Version II. High-Temperature Combustion Reaction Model of H_2/CO/C1-C4 Compounds. http://ignis.usc.edu/USC_Mech_ II.htm.